

1 Evolutionary processes make invasion speed
2 difficult to predict

3 Ben L. Phillips^{1,2}

4 January 6, 2015

5 1. Department of Biosciences, University of Melbourne, Victoria, Australia.

6 2. Centre for Tropical Biodiversity and Climate Change, School of Marine and
7 Tropical Biology, James Cook University, Townsville, Australia.

8 Revised manuscript for consideration in *Biological Invasions*

Article type: Original Article
Word count (Abstract): 245
Word count (Main): 3895
Number of references: 43

9 Keywords: *Genetic drift, Invasive species, Mutation surfing, Spatial sorting,*
10 *Uncertainty, Climate change*

11 **1 Abstract**

12 A capacity to predict the spread rate of populations is critical for understanding
13 the impacts of climate change and invasive species. Despite sophisticated theory de-
14 scribing how populations spread, the prediction of spread rate remains a formidable
15 challenge. As well as the inherent stochasticity in the spread process, spreading
16 populations are subject to strong evolutionary forces (operating on dispersal and
17 reproductive rates) that can cause accelerating spread. Despite these strong evolu-
18 tionary forces, serial founder events and drift on the expanding range edge mean that
19 evolutionary trajectories in the invasion vanguard may be highly stochastic. Here I
20 develop a model of spatial spread in continuous space that incorporates evolution of
21 continuous traits under a quantitative genetic model of inheritance. I use this model
22 to investigate the potential role of evolution on the variation in spread rate between
23 replicate model realisations. Models incorporating evolution exhibited more than
24 four times the variance in spread rate across replicate invasions compared with non-
25 evolving scenarios. Results suggest that the majority of this increase in variation is
26 driven by evolutionary stochasticity on the invasion front rather than initial founder
27 events: in many cases evolutionary stochasticity on the invasion front contributed
28 more than 90% of the variance in spread rate over 30 generations. Our uncertainty
29 around predicted spread rates – whether for invasive species or those shifting under
30 climate change – may be much larger than we expect when the spreading population

³¹ contains heritable variation in rates of dispersal and reproduction.

32 **2 Introduction**

33 Predicting the spread rate of biological invasions has been a longstanding interest of
34 ecologists (Skellam, 1951; Elton, 1958; Hengeveld, 1989). Predicting spread rate is
35 useful for the management of invasive species, but is also fundamental to understand-
36 ing the dynamics of range shift in response to climate change, both past and present
37 (Shigesada and Kawasaki, 1997; Clark et al., 1998; Sax et al., 2005). Increasingly,
38 it is also appreciated that understanding the dynamics of spread may also be im-
39 portant to medicine; in understanding tumour growth and the formation of biofilms
40 (Orlando et al., 2013; van Ditmarsch et al., 2013). Despite these new applications,
41 the long-standing interest of ecologists, and the development of elegant and sophis-
42 ticated theory around the dynamics of spreading populations (e.g., Hastings, 1996),
43 our capacity to forecast spread rate remains poor (Hastings et al., 2005).

44 There is, perhaps, little surprise in this observation. The process of range shift
45 results, after all, from the interplay of two stochastic processes intrinsic to the pop-
46 ulation: dispersal and population growth. These intrinsic processes are, in turn,
47 affected by spatial and temporal variation in the environment. Thus, we should not
48 be surprised that there will always be fundamental limits to our capacity to forecast
49 spread rate. Indeed, even in controlled environments, replicated invasions exhibit
50 wildly varying spread rates (Melbourne and Hastings, 2009).

51 In recent years it has also become apparent that some of our failure to predict

52 spread rate – particularly in situations of accelerating spread – is likely the result
53 of rapid evolution (Travis and Dytham, 2002; Phillips et al., 2008). The process
54 of spread creates powerful selective forces that favour individuals on the invasion
55 front with higher dispersal and reproductive rates (Phillips et al., 2010; Shine et al.,
56 2011; Benichou et al., 2012; Kubisch et al., 2013). These selective forces can, on
57 ecologically-relevant timescales, alter phenotypes on invasion fronts resulting in ac-
58 celerating spread (Perkins, 2012; Perkins et al., 2013).

59 As well as the realisation that rapid evolution can cause profound shifts in spread
60 rate, we are also beginning to appreciate that evolution on invasion fronts can also
61 be highly stochastic (Excoffier and Ray, 2008; Excoffier et al., 2009). The process of
62 range shift creates a situation of serial founder events — only relatively few individu-
63 als make up the invasion vanguard each generation — that can see even maladaptive
64 alleles ‘surf’ to high frequency and be smeared across the invaded range (Klopfstein
65 et al., 2006; Travis et al., 2007). This situation of serial foundering is akin to ge-
66 netic drift: it is drift through space rather than time (Slatkin and Excoffier, 2012).
67 The resulting accumulation of deleterious alleles on invasion fronts has recently been
68 termed “expansion load” and is currently the focus of intense theoretical interest
69 (Peischl et al., 2013).

70 Thus, rapid evolution can drive important variation in spread rate, but the ulti-
71 mate evolutionary trajectory of a spreading population is subject to a high degree

72 of stochasticity through both an initial founder event at colonisation and then serial
73 founder events happening on the invasion front every generation. It remains possible,
74 therefore, that this evolutionary stochasticity contributes to the variation in spread
75 rates we see in nature and in replicated invasion in the lab. To test this idea, I
76 develop an individual-based simulation model that allows both dispersal and repro-
77 ductive rate to evolve. Analysis of this model suggests that evolutionary process can
78 lead to a massive increase in the variability of realised spread rates.

79 **3 Methods**

80 To examine the contributions of various stochastic forces to variation in range shift,
81 I develop a discrete-time simulation model of population and evolutionary dynamics.
82 The model tracks sexually hermaphroditic individuals that shift and reproduce over
83 time in continuous space. I use a quantitative genetics model for the inheritance of
84 two continuous traits: one affecting dispersal and the other affecting fitness. The
85 model is developed and analysed primarily in 1-dimensional space, with a brief ex-
86 tension to the 2-dimensional case. All numerical procedures were conducted in R (R
87 Development Core Team, 2012), and the code is available as an online supplement
88 to this paper (Appendix S2).

89 Individuals express two phenotypes, one relevant to dispersal z_d , and one relevant
90 to fitness z_w . Both traits are continuous (both $\in \mathbb{R}$) with an underlying quantitative

91 genetic structure that assumes trait genetic covariances are zero (there is no genetic
92 correlation between the traits). By taking the individual-based approach, demo-
93 graphic stochasticity and the evolution of trait means and variances can be easily
94 incorporated. Because it is impractical to completely explore parameter space in
95 such a model, however, I take the approach of providing a proof-of-concept; demon-
96 strating the potential importance of evolutionary process in generating both rapid
97 and less predictable invasion speeds. An analytical treatment of these ideas remains
98 a formidable challenge.

99 **3.1 Population dynamics**

100 Generations are discrete and non-overlapping. Local dynamics are determined by
101 reference to a continuous spatial “neighbourhood” whose size remains constant. Both
102 the density of individuals and the mean and variance of trait values in an individual’s
103 neighbourhood are calculated as a sum or mean across the entire population weighted
104 for distance from the individual. The weighting through space is simply a Gaussian
105 probability density function with a standard deviation set to one. Thus, local density
106 at location x , n_x , is given as a sum over the p individuals in the population:

$$n_x = \sum_{i=1}^p N(d_{i,x}, \sigma) \quad (1)$$

107 Where $N()$ is the Gaussian pdf, $d_{i,x}$ is the distance between individual i and

108 location x , and σ is the smoothing scale (a constant; standard deviation = 1 in
109 this case). The smoothing scale (the scale of local dynamics) is independent of
110 dispersal values in the population. This choice effectively sets up a reproductive
111 phase (in which local interactions matter) and a dispersal phase (in which local
112 interactions do not matter). The smoothing scale, in conjunction with the population
113 carrying capacity (n^* , see below) together define the approximate neighbourhood size
114 ($= 4n^*\sigma$) of demes within the population.

115 Individual reproduction is a stochastic density-dependent process. I calculate
116 an expected number of offspring for each individual $E(o_i)$ using the Beverton-Holt
117 (Beverton and Holt, 1957) population growth function $E(o_i) = \frac{R_i}{1+an_{i,x}}$. Where R_i is
118 an individual's expected density-independent fecundity (determined by its z_w pheno-
119 type, see below), $n_{i,x}$ is the density at the individual's location, and a is a constant
120 that determines the strength of intraspecific competition. At the beginning of sim-
121 ulations, a is set to $a = \frac{R_{max}-1}{n^*}$ where R_{max} is the maximum expected fecundity
122 achievable by an individual in the population, and n^* is the carrying capacity that
123 would be achieved if all individuals achieved a fecundity of R_{max} .

124 A subset of simulations also involved a strong Allee effect. To achieve the Allee
125 effect, I simply multiplied R_i by $\frac{n_x}{0.5+n_x}$, which produces inverse density dependence
126 at low population densities (Stephens and Sutherland, 1999). Irrespective, once an
127 expected number of offspring is calculated, the realised number of offspring is drawn

128 from a Poisson distribution with mean of $E(o_i)$. Beverton-Holt dynamics have the
129 useful property that population dynamics remain stable irrespective of the population
130 growth rate. This choice of local dynamic ensures that local population fluctuations
131 are purely due to demographic stochasticity.

132 Following reproduction, all parents die and offspring disperse. Individuals dis-
133 perse according to a draw from a Gaussian distribution with a mean of zero and a
134 standard deviation given by $e^{z_{d,i}}$, where $z_{d,i}$ is the individual's dispersal phenotype.

135 **3.2 Trait evolution**

136 Individuals express two phenotypes, one, z_w , that determines the individual's maxi-
137 mum expected reproductive rate, and the other, z_d , that determines the individual's
138 dispersal propensity. An individual's reproductive rate is influenced by how well
139 adapted it is to the local environment, where the optimum value for z_w is 0. The
140 density-independent fecundity of an individual, R_i , is a function of an individual's
141 z_w as,

$$R_i = R_{max} e^{-kz_{w,i}^2} \quad (2)$$

142 where R_{max} is the upper limit on expected individual fecundity (constant across
143 individuals), and k is a constant defining the strength of stabilising selection in the
144 system (here set to a constant value of 2).

145 The inheritance of traits is determined by a basic quantitative genetic model in
146 which individuals mate with a partner drawn at random (with probability weighted
147 by $N(d_{i,x}, \sigma)$) from the population. All individuals reproduce and each individual
148 carries a “breeding value” that contributes to the phenotype of its offspring. In
149 quantitative genetics, an individual’s breeding value represents the sum of the addi-
150 tive genetic contributions to its phenotype and is usually estimated from the mean
151 of its offspring (Lynch and Walsh, 1998). Instead of estimating breeding values, I
152 define them here for each individual before its offspring are produced. Importantly,
153 the variance in breeding values in a randomly mating population is identical to the
154 additive genetic variance in that population (Lynch and Walsh, 1998), so initially,
155 each individual’s breeding value can be determined by a draw from a normal distri-
156 bution with mean set to the trait mean and variance equal to the additive genetic
157 variance of the population V_a (see below). Offspring breeding values are then cen-
158 tered on the resulting mid-parent breeding value (the mean of the breeding values of
159 the parents), but deviate from this mid-parent value according to a normal distribu-
160 tion with variance equal to half the variance in local mean breeding values (i.e., half
161 the local additive variance). This distribution of offspring breeding values is that
162 expected in a situation with no dominance or epistasis (Roughgarden, 1979), and
163 largely reflects variance between offspring driven by segregation (i.e., randomness in
164 the set of parental alleles inherited by each offspring). Thus, for example, the breed-

165 ing value for dispersal of offspring one from parent one at location x is calculated
166 as,

$$b_{d,o1,x} \sim N\left(\frac{b_{d,1,x} + b_{d,2}}{2}, \sqrt{\frac{V_{a,d,x}}{2}}\right).$$

167 Local trait mean breeding values ($\bar{b}_{d,x}$ and $\bar{b}_{w,x}$) and variances are calculated over
168 the same spatial neighbourhood as that governing local dynamics. For example (for
169 b_d),

$$\bar{b}_{d,x} = \frac{1}{n_x} \sum_{i=1}^p b_{d,i} N(d_{i,x}, \sigma) \quad (3)$$

170 and local trait genetic variances are calculated as,

$$V_{a,d,x} = \frac{1}{n_x} \sum_{i=1}^p (b_{d,i} - \bar{b}_{d,x})^2 N(d_{x,i}, \sigma) \quad (4)$$

171 Thus, I only track standing variation: genetic variances evolve through space as a
172 consequence of gene flow (movement of individuals), and are eroded by selection, but
173 are not subject to the additional inflationary force of mutation. The modelled sce-
174 nario focusses on small population sizes and short-term dynamics in which mutational
175 contributions to variance are likely to be negligible. The offspring's final phenotype
176 (z_d, z_w) is determined by adding environmental variance (V_e) to the breeding values
177 again using a random draw from a Gaussian distribution. For example,

$$z_{d,i} \sim N(b_{d,i}, \sqrt{V_{e,d}}).$$

178 V_e is constant over time and space: when the model is initiated, the amount of
179 environmental variance added to offspring breeding value is determined according to
180 the trait's heritability h^2 and total phenotypic variance, V_p , where $V_p = V_e + V_a$ and
181 $V_a = h^2 V_p$ and .

182 To keep spread rate modest (and computationally tractable), I set the initial
183 phenotypic mean of z_d to $\ln(4)$ (a root mean square displacement of 4 units) and the
184 initial total phenotypic variance of z_d to 0.2 in all simulations. At initialisation, then,
185 the average individual will leave it's local neighbourhood (defined as ± 2 units from
186 its location). The initial mean z_w phenotype was set to zero (the optimum value)
187 and again total phenotypic variance was set to 0.2.

188 **3.3 The modelled scenario**

189 All simulations begin with the introduction of 20 individuals to a point in space, and
190 the model examines variation in realised spread distances over 30 generations. For
191 the 1-dimensional case, I examined values of n^* between 10-50, and R_{max} between
192 2-20. At the end of these 30 generations, the distance spread (the distance between
193 introduction and the location of the furthest individual) is recorded for both invasion
194 fronts (Fig. 1). Recording spread distance of the twin invasion fronts allows me to

195 calculate a within-population measure of variation in spread rate.

196 For each set of parameters examined, I created 20 founder populations (each
197 containing 20 individuals). For each founder population of 20 individuals, 20 replicate
198 realisations of an invasion were undertaken: ten with trait heritabilities set to zero,
199 and ten with trait heritabilities set to 0.3. For each of these replicates, spread
200 distance was recorded for both invasion fronts. Initial trait variances were kept
201 identical between the evolving and non-evolving scenarios (although trait variances
202 then evolved in the evolving scenario as V_a evolves). With this arrangement of
203 replicated invasions, I can partition variation in spread distance into that resulting
204 from,

- 205 1. stochasticity in dispersal and demography (the total variance – within and
206 across populations – in spread distance in the non-evolving populations), S_0 .
207 Noting that founder events do not occur in the non-evolving scenario, because
208 the traits are not heritable;
- 209 2. initial founder events (the between-population variance in spread distance in
210 the evolving populations), S_f ; and
- 211 3. stochasticity in the evolutionary process (the within-population variance in
212 spread distance in the evolving populations, S_e , minus that due to pure demo-
213 graphic stochasticity, S_0).

214 The 2-dimensional case was substantially more computationally intensive, so for
215 this case I only examined one value of n^* ($n^* = 10$), and only examined a smaller
216 range of R_{max} (between 2-10). I otherwise kept the design the same as the 1-
217 dimensional case (Fig. 2). The other difference for the 2-dimensional simulations
218 was that measurements of spread distance were taken along both the x , and y axes:
219 individuals' locations in (x, y) were collapsed onto each axis yielding two sets of twin
220 invasion fronts. Other than generating twice as many within-population measures of
221 spread rate, subsequent analysis proceeded as per the 1-dimensional case.

222 4 Results

223 4.1 1-dimensional situation

224 The model deliberately investigated very short time periods (30 generations of spread)
225 and focussed on realistic trait heritabilities (usually = 0.3). Despite the short spread
226 time and the modest heritability (=0.3), models with heritable traits resulted in
227 greater spread rates (Fig. 3). When heritability was 0.3, spread rates were, on av-
228 erage across all simulations, 1.3 times faster. Although evolution resulted in spread
229 rates 1.3 times faster than the non-evolving scenario, the variance in spread rate
230 was, on average, 4.2 times larger in the evolutionary scenarios (Fig. 3). Importantly,
231 much of this additional variation manifested as variation within a single realisation of

232 spread: i.e., large differences in the spread rate between the twin invasion fronts (see
233 e.g., Fig. 1). That is, there were typically differences in the evolutionary trajectory
234 on the twin invasion fronts.

235 Why did these differences emerge? In this model, the signal of phenotype surfing
236 (driven by serial founder events) was evident in the fitness trait, which often showed
237 substantial deviations from optimal values (i.e., zero) on the advancing range mar-
238 gins. That is, serial founder events clearly undermine the stabilising selection op-
239 erating on this trait. This same phenotype surfing must also have occurred for the
240 dispersal trait, although this trait was subject to strong directional evolution (driven
241 by spatial sorting and natural selection, see Phillips et al. (2010)), and so in this
242 case surfing manifests as differing rates of evolutionary shift. Acting on both traits
243 together, serial founder events (“surfing”) resulted in strong disparities in the evolved
244 spread rate on each of the twin invasion fronts. The “final” dispersal and fitness val-
245 ues on each front will determine the equilibrium spread rate (Fisher, 1937; Benichou
246 et al., 2012), so these varying evolutionary trajectories caused substantial variation
247 in spread rate between twin invasion fronts.

248 Overall, this evolutionary stochasticity typically contributed to most (often more
249 than 90%) of the variance in spread rate in the 1-dimensional model (Fig. 3), with
250 much lower levels of variance being attributable to pure demographic stochasticity
251 and the initial founder effect (Fig. 3). This basic result appears reasonably robust to

252 variation in the equilibrium population density (n^*) and maximum fecundity (R_{max} ,
253 Fig. 3). Demographic stochasticity did, however, play a larger role when intrinsic
254 rates of population growth (R_{max}) were low, and when trait heritability was low
255 (Appendix S1). Interestingly, the inclusion of a strong Allee effect lowered the overall
256 stochasticity in spread rate, but did not greatly alter the proportional contributions
257 of demography, initial founder effect, and evolution (Appendix S1).

258 4.2 2-dimensional situation

259 Here again, models with heritable variation resulted in faster spread rates (Fig. 4).
260 This increased spread rate for the 2D case was similar to that for the 1D case. If
261 we compare the overall increase in spread due to evolution between the two spaces
262 (bearing in mind that we can only use a subset of the 1D cases for comparison:
263 $R_{max} = \{2, 4, 6, 8, 10\}$ and $n^* = 10$) then the ratio of proportional increase in spread
264 rate 1D:2D is 1.21:1.16. As with the 1D case, overall variance in spread rate was
265 substantially higher for the evolved scenario (Fig. 4) but, this increase was more
266 modest in the 2D case compared with the equivalent parameter settings in the 1D
267 case: the ratio of proportional increase in variance, 1D:2D was 2.52:1.84.

268 As with the 1D case, much of this increased variance in spread rate manifested
269 as variation within a single realisation of spread. That is, there were substantial
270 differences in spread rate between different sectors of the invasion and these dif-

271 ferences were driven by differing evolutionary trajectories on various parts of the
272 invasion front (Figs 2 and 4). Thus, although, the overall increase in variation in
273 spread rate was smaller in the 2D case compared with the 1D case, the proportional
274 contributions of demography, initial founder event, and evolutionary stochasticity,
275 were similar: evolutionary stochasticity typically generated more than 90% of the
276 observed variation in spread rate.

277 **5 Discussion**

278 If we are to accurately forecast rates of spread, whether for toads, tumours, or
279 trees, it is clear that we need to account for variation in dispersal and reproduction
280 (e.g., Neubert et al., 2000; Schreiber and Ryan, 2011). In purely ecological models
281 of spread (i.e., those that do not incorporate evolution) demographic stochasticity
282 can act to either slow (e.g., Lewis, 2000; Snyder, 2003) or increase (e.g., Ellner and
283 Schreiber, 2012) spread rates relative to deterministic expectations. Evolutionary
284 models of spread, on the other hand, typically lead to higher rates of spread than
285 those predicted by equivalent ecological models because dispersal and reproductive
286 rates evolve upwards during range advance (Burton et al., 2010; Phillips et al., 2010;
287 Perkins et al., 2013). My analysis now suggests that evolutionary processes not only
288 make invasions faster, they also make invasion speed more unpredictable, because
289 very different spread rates can emerge from identical starting conditions.

290 It appears that much of this variation in spread rate might be due to evolutionary
291 stochasticity: evolutionary processes pushing through a strong stochastic filter. This
292 evolutionary stochasticity is a result of the serial founder events that occur on the
293 invasion front each generation. Clearly, the analysis here is not exhaustive: an infinite
294 parameter space exists within the model and exploring it all is not practicable. Thus,
295 I aim mostly for a proof-of-concept: to demonstrate that evolutionary stochasticity
296 might play an important role in making invasions inherently difficult to forecast, and
297 that it can do so across a wide range of circumstances. The work complements recent
298 work by Peischl et al. (2015) which shows that the accumulation of fitness-reducing
299 variants on an expanding range edge can limit the rate of spread. Here, I show that
300 both dispersal and fitness traits are affected by serial foundering, and the consequent
301 evolutionary stochasticity in spread rate is substantial. Indeed, the large role of
302 evolutionary stochasticity appears to be a robust result: evolutionary stochasticity
303 is associated with more than 90% of the variation in spread rate, in both one and two
304 dimensions and across a large range of reproductive rates, equilibrium densities, and
305 heritabilities. By contrast, other processes acting alone — demographic stochasticity
306 and initial foundering — often account for relatively minor proportions of the overall
307 variance in spread rate (Figs 3 and 4).

308 Clearly, however, the degree to which evolutionary stochasticity makes invasions
309 unpredictable will depend on the system at hand. One constraint with this system is

310 that, for logistical reasons, the population densities I have used are relatively mod-
311 est (at $n^* = 50$, for example neighbourhood size is approximately 200 individuals
312 with continuous gene flow between demes), and so we might expect drift to be an
313 important force in this system, even at equilibrium. Nonetheless, varying n^* made
314 little difference to the proportion of variance attributable to evolutionary stochastic-
315 ity (see lower panel of Fig. 3). This is exactly what we would expect if evolutionary
316 dynamics were dominated by conditions on the leading edge of the invasion. Pop-
317 ulation densities on this leading edge are low and serially founded irrespective of
318 the equilibrium density; so varying n^* makes little difference to the degree of drift
319 on the invasion front.

320 The model here also shows that absolute variance in spread rate is much larger in
321 a 1D space compared with the 2D case. Stochastic effects are exaggerated in the 1D
322 case because serial founder events are not moderated by the spatial autocorrelation
323 that acts across another spatial dimension. In other words the effect of drift on the
324 invasion front is lower in the 2D case. As well as reducing the strength of the serial
325 founder effect, in two dimensions, gene flow perpendicular to the direction of invasion
326 should eventually ensure that a close-to-optimal invasion phenotype emerges across
327 the entire invasion front (see Hallatschek et al., 2007). But although this should
328 happen, it will take time. In two dimensions, and given sufficient time, we would
329 expect different rates of invasion to emerge across different sectors of the invasion.

330 These different rates will remain stable for a period of time before being invaded
331 (from the side) by sets of phenotypes that generate more rapid invasion speed (a
332 phenomenon apparent in Fig 2).

333 Another spatial dimension might also alter the evolutionary effect by slowing
334 down the erosion of genetic variance that occurs very rapidly in the 1D case. A
335 slower loss of variance would likely allow the stochastic aspects of the evolutionary
336 process more time to play out; giving vanguard populations more time to drift. The
337 decay of genetic variance could also be slowed by allowing greater capacity for long-
338 distance dispersal. Long-distance dispersal, because it creates greater mixing, has
339 been shown to slow the loss of genetic variance on invasion fronts (e.g., Bialozyt
340 et al., 2006). Thus, swapping the Gaussian dispersal kernel used here for one with
341 fatter tails would slow the loss of genetic variance on the invasion front and, because
342 of this, potentially increase the proportion of variance in spread rate contributed by
343 evolutionary stochasticity. More generally, the shape of the dispersal kernel is already
344 known to have a major impact on invasion dynamics (Kot et al., 1996). Highly
345 leptokurtic kernels, for example, can result in patchy and highly stochastic invasions
346 (Lewis and Pacala, 2000; Bocedi et al., 2014) — a situation where serial founder
347 events might be particularly pronounced. Thus, the shape of the dispersal kernel
348 remains a critical consideration for both the ecological and evolutionary dynamics of
349 invasion.

350 The model I explore also treats the environment as homogenous in space and time.
351 Adding stochastic environmental variation to the model would presumably increase
352 the role of “demographic” stochasticity in generating variance in spread rates. Even
353 so, it is likely that evolutionary stochasticity will still play a strong role in making
354 spread rate unpredictable. The reason for this is that evolution generates autocorre-
355 lated variation in dispersal and demographic rates: this autocorrelation emerges in
356 the evolutionary model simply because traits are heritable. The work of Schreiber
357 and Ryan (2011) clearly shows that autocorrelated demographic stochasticity in-
358 creases the overall unpredictability of spread rate above that seen when stochasticity
359 is not autocorrelated. Thus, even in a model with strong environmental stochasticity,
360 we would expect evolutionary effects to make spread rate even more unpredictable.

361 Finally, the introduction of an Allee effect reduces both evolutionary and de-
362 mographic stochasticity. By forcing the vanguard population to grow from a larger
363 founder population each generation, Allee effects reduce demographic stochasticity
364 and also slow the loss of genetic variation in the vanguard (Taylor and Hastings, 2005;
365 Hallatschek and Nelson, 2008). As well as this, by creating a negative correlation
366 between fitness and dispersal on the invasion front, Allee effects can undermine the
367 evolutionary processes that lead to increasing dispersal and reproductive rates (e.g.,
368 Travis and Dytham, 2002; Phillips, 2009; Burton et al., 2010). As a consequence,
369 Allee effects may play a particularly powerful role in decreasing overall stochasticity

370 during invasion. Indeed, when I incorporated an Allee effect, the model showed much
371 lower overall stochasticity in spread distance although, again, the proportion of this
372 variance due to evolutionary stochasticity remained high (Appendix S1).

373 There are, of course, other ways in which the role of evolutionary stochasticity
374 during invasion can be diminished. Most obviously, if there is no genetic variance
375 for the traits that determine spread rate (reproductive and dispersal rates), evolu-
376 tionary stochasticity will not be an issue. Where there is even a small amount of
377 heritable variance in dispersal and reproductive rates, however, my analysis suggests
378 that evolutionary stochasticity can play a powerful role in generating unpredictable
379 invasion speeds. Obviously, extrinsic factors (e.g., environmental heterogeneity, or
380 species interactions) will still play an important role (e.g., Tobin et al., 2007; Burton
381 et al., 2010), but the analysis here suggests that a great deal of variance in spread
382 rate may be explainable by intrinsic properties of the population, without the need
383 to invoke variation in the environment. This observation is at once encouraging —
384 environmental variation may be less important than we currently think — and dis-
385 couraging, because to be clear about our predictive uncertainty requires information
386 on population attributes that are difficult to measure (e.g., trait heritabilities). What
387 is clear, however, is that evolutionary processes — both deterministic and stochastic
388 — are of critical importance in predicting invasion speed and in understanding our
389 uncertainties around these predictions.

390 **6 Acknowledgements**

391 The idea for this paper came whilst preparing a talk for a conference on “Biological
392 invasions and evolutionary biology, stochastic and deterministic models” in Lyon,
393 2013. So I thank the organisers of the conference — Jean Bérard, Vincent Calvez,
394 and Gaël Raoul — for both the conference and their invitation. I also thank Wayne
395 Mallet and Jeremy Vanderwal for ongoing technical support around High Perfor-
396 mance Computing. Funding for this work was provided by the Australian Research
397 Council (DP1094646).

398 **References**

- 399 Benichou, O., V. Calvez, N. Meunier, and R. Voituriez, 2012. Front acceleration by
400 dynamic selection in Fisher population waves. *Physical Review E* 86:041908. URL
401 <http://pre.aps.org/abstract/PRE/v86/i4/e041908>.
- 402 Beverton, R. J. H. and S. J. Holt, 1957. On the dynamics of exploited fish popula-
403 tions, vol. 19. UK Ministry of Agriculture.
- 404 Bialozyt, R., B. Ziegenhagen, and R. J. Petit, 2006. Contrasting ef-
405 fects of long distance seed dispersal on genetic diversity during
406 range expansion. *Journal of evolutionary biology* 19:12–20. URL
407 <http://www.ncbi.nlm.nih.gov/pubmed/16405572>.

408 Bocedi, G., S. C. Palmer, G. Pe'er, R. K. Heikkinen, Y. G. Matsinos,
409 K. Watts, and J. M. Travis, 2014. RangeShifter: a platform for mod-
410 elling spatial eco-evolutionary dynamics and species' responses to environ-
411 mental changes. *Methods in Ecology and Evolution* 5:388–396. URL
412 <http://doi.wiley.com/10.1111/2041-210X.12162>.

413 Burton, O. J., J. M. J. Travis, and B. L. Phillips, 2010. Trade-offs and the evolution
414 of life-histories during range expansion. *Ecology Letters* 13:1210–1220.

415 Clark, J. S., C. Fastie, G. Hurtt, S. T. Jackson, C. Johnson, G. A. King, M. Lewis,
416 J. Lynch, S. Pacala, C. Prentice, E. W. Schupp, T. Webb III, P. Wyckoff, T. Webb,
417 and A. King, 1998. Reid's paradox of rapid plant migration. *BioScience* 48:13–24.

418 van Ditmarsch, D., K. E. Boyle, H. Sakhtah, J. E. Oyler, C. D. Nadell, E. Déziel, L. E.
419 Dietrich, and J. B. Xavier, 2013. Convergent Evolution of Hyperswarming Leads
420 to Impaired Biofilm Formation in Pathogenic Bacteria. *Cell Reports* 4:697–708.
421 URL <http://linkinghub.elsevier.com/retrieve/pii/S2211124713003884>.

422 Ellner, S. and S. Schreiber, 2012. Temporally variable dis-
423 persal and demography can accelerate the spread of invad-
424 ing species. *Theoretical Population Biology* 82:283–298. URL
425 <http://www.sciencedirect.com/science/article/pii/S0040580912000445>.

426 Elton, C. S., 1958. *The ecology of invasions by animals and plants*. Methuen, London.

427 Excoffier, L., M. Foll, and R. J. Petit, 2009. Genetic Consequences of Range Ex-
428 pansions. *Annual Review of Ecology, Evolution, and Systematics* 40:481–501. URL

429 <http://arjournals.annualreviews.org/doi/abs/10.1146/annurev.ecolsys.39.110707.17341>

430 Excoffier, L. and N. Ray, 2008. Surfing during population expansions promotes
431 genetic revolutions and structuration. *Trends in Ecology & Evolution* 22:347–351.

432 Fisher, R. A., 1937. The wave advance of advantageous genes. *Annals of Eugenics*
433 7:355–369.

434 Hallatschek, O., P. Hersen, S. Ramanathan, and D. R. Nelson, 2007. Ge-
435 netic drift at expanding frontiers promotes gene segregation. *Proceedings of the*

436 *National Academy of Sciences of the United States of America* 104:19926–30. URL

437 [http://www.pubmedcentral.nih.gov/articlerender.fcgi?artid=2148399&tool=pmcentrez&re](http://www.pubmedcentral.nih.gov/articlerender.fcgi?artid=2148399&tool=pmcentrez&rendition=full)

438 Hallatschek, O. and D. R. Nelson, 2008. Gene surfing in expand-
439 ing populations. *Theoretical population biology* 73:158–70. URL

440 <http://www.ncbi.nlm.nih.gov/pubmed/17963807>.

441 Hastings, A., 1996. Models of spatial spread: A synthesis. *Biological Conservation*
442 78:143–148. URL <Go to ISI>://A1996VP46800012.

443 Hastings, A., K. Cuddington, K. F. Davies, C. J. Dugaw, S. Elmendorf, A. Free-
444 stone, S. Harrison, M. Holland, J. Lambrinos, U. Malvadkar, B. A. Melbourne,

- 445 K. Moore, C. Taylor, and D. Thomson, 2005. The spatial spread of invasions: new
446 developments in theory and evidence. *Ecology Letters* 8:91–101.
- 447 Hengeveld, R., 1989. *Dynamics of biological invasions*. Chapman and Hall, New
448 York.
- 449 Klopstein, S., M. Currat, and L. Excoffier, 2006. The fate of mutations surfing on
450 the wave of range expansion. *Molecular Biology and Evolution* 23:482–490.
- 451 Kot, M., M. A. Lewis, P. VandenDriessche, and P. Van Den Driessche, 1996.
452 Dispersal data and the spread of invading organisms. *Ecology* 77:2027–
453 2042. URL <http://www.esajournals.org/doi/abs/10.2307/2265698> <Go to
454 ISI>://A1996VM42100008.
- 455 Kubisch, A., E. a. Fronhofer, H. J. Poethke, and T. Hovestadt, 2013. Kin Competi-
456 tion as a Major Driving Force for Invasions. *The American Naturalist* 181:700–706.
457 URL <http://www.jstor.org/stable/info/10.1086/670008>.
- 458 Lewis, M., 2000. Spread rate for a nonlinear stochastic in-
459 vasion. *Journal of Mathematical Biology* 41:430–454. URL
460 <http://link.springer.com/article/10.1007/s002850000022>.
- 461 Lewis, M. and S. Pacala, 2000. Modeling and analysis of stochastic in-
462 vasion processes. *Journal of Mathematical Biology* 41:387–429. URL
463 <http://link.springer.com/article/10.1007/s002850000050>.

464 Lynch, M. and B. Walsh, 1998. *Genetics and Analysis of Quantitative Traits*. Sinauer
465 Associates, Sunderland, MA.

466 Melbourne, B. a. and A. Hastings, 2009. Highly variable spread rates in replicated
467 biological invasions: fundamental limits to predictability. *Science* (New York,
468 N.Y.) 325:1536–9. URL <http://www.ncbi.nlm.nih.gov/pubmed/19762641>.

469 Neubert, M. G., M. Kot, and M. a. Lewis, 2000. Invasion speeds in fluctuating envi-
470 ronments. *Proceedings. Biological sciences / The Royal Society* 267:1603–10. URL
471 <http://www.pubmedcentral.nih.gov/articlerender.fcgi?artid=1690727&tool=pmcentrez&rendition=full>

472 Orlando, P. a., R. a. Gatenby, and J. S. Brown, 2013. Tumor Evo-
473 lution in Space: The Effects of Competition Colonization Tradeoffs
474 on Tumor Invasion Dynamics. *Frontiers in Oncology* 3:1–12. URL
475 http://www.frontiersin.org/Molecular_and_Cellular_Oncology/10.3389/fonc.2013.00045/a

476 Peischl, S., I. Dupanloup, M. Kirkpatrick, and L. Excoffier, 2013. On the accu-
477 mulation of deleterious mutations during range expansions. *Molecular ecology*
478 22:5972–82. URL <http://www.ncbi.nlm.nih.gov/pubmed/24102784>.

479 Peischl, S., M. Kirkpatrick, and L. Excoffier, 2015. Expansion load and the evolu-
480 tionary dynamics of a species range. *American Naturalist* in press.

481 Perkins, T. A., 2012. Evolutionarily labile species interactions and spatial spread of
482 invasive species. *The American Naturalist* 179:E37–E54.

483 Perkins, T. A., B. L. Phillips, M. L. Baskett, and A. Hastings, 2013. Evolution
484 of dispersal and life-history interact to drive accelerating spread of an invasive
485 species. *Ecology Letters* in press.

486 Phillips, B., G. Brown, and R. Shine, 2010. Life-history evolu-
487 tion in range-shifting populations. *Ecology* 91:1617–1627. URL
488 <http://www.esajournals.org/doi/abs/10.1890/09-0910.1?ai=rv&af=R>.

489 Phillips, B. L., 2009. The evolution of growth rates on an expanding range edge.
490 *Biology Letters* 5:802–804. URL <Go to ISI>://000271632000026.

491 Phillips, B. L., G. P. Brown, J. M. J. Travis, and R. Shine, 2008.
492 Reid’s paradox revisited: the evolution of dispersal kernels during
493 range expansion. *The American naturalist* 172 Suppl:S34–48. URL
494 <http://www.ncbi.nlm.nih.gov/pubmed/18554142>.

495 R Development Core Team, 2012. R: A language and environment for statistical
496 computing. URL <http://www.r-project.org>.

497 Roughgarden, J. E., 1979. *Theory of population genetics and evolutionary ecology:*
498 *an introduction*. Macmillan, New York.

499 Sax, D. F., J. J. Stachowicz, and S. D. Gaines, 2005. *Species invasions: insights into*
500 *ecology, evolution, and biogeography*.

501 Schreiber, S. J. and M. E. Ryan, 2011. Invasion speeds for structured pop-
502 ulations in fluctuating environments. *Theoretical Ecology* 4:423–434. URL
503 <http://link.springer.com/10.1007/s12080-010-0098-5>.

504 Shigesada, N. and K. Kawasaki, 1997. *Biological invasions: theory and practice*.
505 Oxford University Press, Oxford.

506 Shine, R., G. P. Brown, and B. L. Phillips, 2011. An evolutionary process that
507 assembles phenotypes through space rather than through time. *PNAS* 108:5708–
508 5711.

509 Skellam, J., 1951. Random dispersal in theoretical populations. *Biometrika* 38:196–
510 218. URL <http://www.springerlink.com/index/13G436H7L4UX38QU.pdf>.

511 Slatkin, M. and L. Excoffier, 2012. Serial founder effects during range ex-
512 pansion: a spatial analog of genetic drift. *Genetics* 191:171–81. URL
513 [http://www.pubmedcentral.nih.gov/articlerender.fcgi?artid=3338258&tool=pmcentrez&re](http://www.pubmedcentral.nih.gov/articlerender.fcgi?artid=3338258&tool=pmcentrez&rend=full)

514 Snyder, R. E., 2003. How Demographic Stochasticity Can
515 Slow Biological Invasions. *Ecology* 84:1333–1339. URL
516 [http://www.esajournals.org/doi/abs/10.1890/0012-9658\(2003\)084\[1333:HDSCSB\]2.0.CO;2](http://www.esajournals.org/doi/abs/10.1890/0012-9658(2003)084[1333:HDSCSB]2.0.CO;2).

517 Stephens, P. and W. Sutherland, 1999. Consequences of the Allee effect for behaviour,
518 ecology and conservation. *Trends in Ecology & Evolution* 17:401–405. URL
519 <http://www.sciencedirect.com/science/article/pii/S0169534799016845>.

520 Taylor, C. M. and A. Hastings, 2005. Allee effects in bi-
521 ological invasions. *Ecology Letters* 8:895–908. URL
522 <http://blackwell-synergy.com/doi/abs/10.1111/j.1461-0248.2005.00787.x>.

523 Tobin, P. C., S. L. Whitmire, D. M. Johnson, O. N. Bjørnstad, and
524 A. M. Liebhold, 2007. Invasion speed is affected by geographical vari-
525 ation in the strength of Allee effects. *Ecology letters* 10:36–43. URL
526 <http://www.ncbi.nlm.nih.gov/pubmed/17204115>.

527 Travis, J. M. J. and C. Dytham, 2002. Dispersal evolution during invasions. *Evolu-*
528 *tionary Ecology Research* 4:1119–1129.

529 Travis, J. M. J., T. Münkemüller, O. J. Burton, A. Best, C. Dytham, and K. Johst,
530 2007. Deleterious mutations can surf to high densities on the wave front of an
531 expanding population. *Molecular Biology and Evolution* 24:2334–2343.

532 **7 Biosketch**

533 Ben Phillips is a QEII Research Fellow at the Department of Biosciences, University
534 of Melbourne, Australia. His work focuses on contemporary evolution: how it plays
535 out in space, and how it interacts with ecology. He has recently become fascinated
536 by range edges and how evolution might affect whether, and how fast, range edges
537 will shift under climate change. <http://blphillipsresearch.wordpress.com>

538 8 Figures

539 **Figure 1.** A typical realisation of the model in 1-dimension following 30 generations
540 of spread. Grey lines represent initial trait value (horizontal line) or introduction
541 location (vertical line). First row: mean and genetic variance of the trait affecting
542 reproductive output (z_w). Initial trait value in this case is zero, and the figure
543 indicates substantial drift from this optimum, moderate erosion of genetic variance at
544 the introduction locale, and substantial loss of genetic variance towards the invasion
545 front. Second row: mean and genetic variance of the trait affecting dispersal (z_d).
546 In this case the two invasion fronts have evolved very different values for the trait,
547 trait variance has increased from initial values at the introduction location, but still
548 decreases strongly towards the invasion front. Third row: population density through
549 space, and mean individual fitness $E(\bar{o})$ through space. The genetic neighbourhood
550 of each individual spans an interval of four units along the x-axis.

551 **Figure 2.** A typical realisation of the model in 2-dimensions. Snapshots at
552 time 5, 15, and 30 generations are shown at each row of the figure panel. The
553 columns of the figure panel correspond to the traits for dispersal z_d and fitness
554 z_w respectively. Colours allow us to observe individual breeding values for these two
555 traits and how these vary over space and time. Note that, like the 1-dimensional case,
556 different evolutionary outcomes emerge on different parts of the invasion front. In
557 the present case higher dispersal values emerge in the upper sector, and lower fitness

558 values emerge on both right and left sectors. Together, these differing evolutionary
559 trajectories lead to differing spread rates (clearly apparent in the lower panel, in
560 which a circle, and crosshairs centred on the starting position, have been placed for
561 reference).

562 **Figure 3.** Spread distances in a 1-dimensional space under scenarios with and
563 without trait evolution. The top panel shows spread distance with and without
564 trait evolution across a range of R_{max} (with $n^*=50$). Shaded areas represent the
565 standard deviation in spread distance across replicate invasion fronts. It is clear
566 that allowing dispersal and reproductive rate to evolve both increases the rate of
567 invasion as well as the variation in that rate across realisations. The second panel
568 shows variance in spread distance decomposed into that resulting from demographic
569 stochasticity, initial founder events, and evolutionary stochasticity. Line thickness
570 in lower two panels represents different values of intraspecific competition (thick to
571 thin; $n^* = 50, 25, 10$ respectively). The lower panel shows this same decomposition
572 of variance as a proportion of total variance. At low rates of population increase
573 ($R_{max} = 2$) demographic stochasticity contributes around 20% of the variance in
574 spread distances in the model. Above these low values of R_{max} , however, stochastic
575 evolutionary processes on the expanding range edge (serial foundering: ‘Evolutionary
576 stochasticity’) accounts for most of the variation in spread distance.

577 **Figure 4.** Spread distances in a 2-dimensional space under scenarios with and

578 without trait evolution. The top panel shows spread distance with and without trait
579 evolution across a range of R_{max} (with $n^*=10$). Shaded areas represent the standard
580 deviation in spread distance across replicate invasion fronts. It is clear that allowing
581 dispersal and reproductive rate to evolve both increases the rate of invasion as well
582 as the variation in that rate across realisations. The second panel shows variance
583 in spread distance decomposed into that resulting from demographic stochasticity,
584 initial founder events, and evolutionary stochasticity (again $n^* =10$ throughout).
585 The lower panel shows this same decomposition of variance as a proportion of total
586 variance. At low rates of population increase ($R_{max} = 2$) demographic stochasticity
587 contributes around 20% of the variance in spread distances in the model. Above these
588 low values of R_{max} , however, stochastic evolutionary processes on the expanding
589 range edge (serial foundering: ‘Evolutionary stochasticity’) accounts for most of the
590 variation in spread distance.

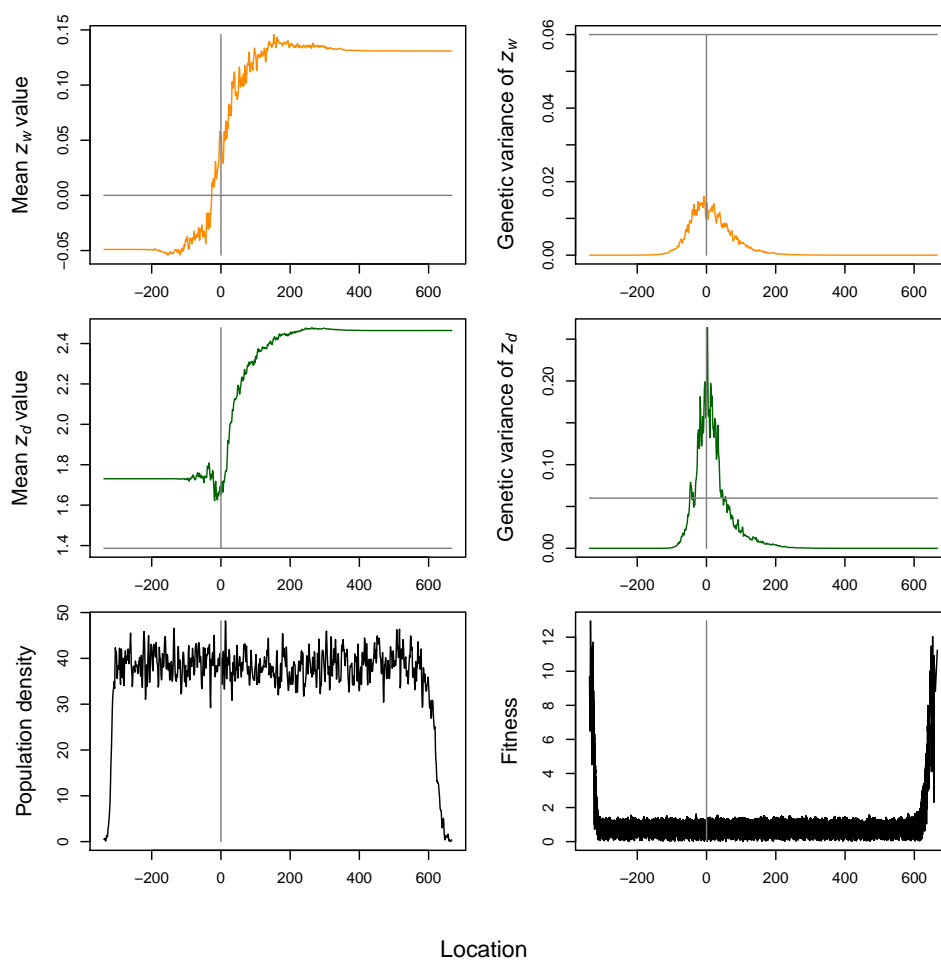


Figure 1:

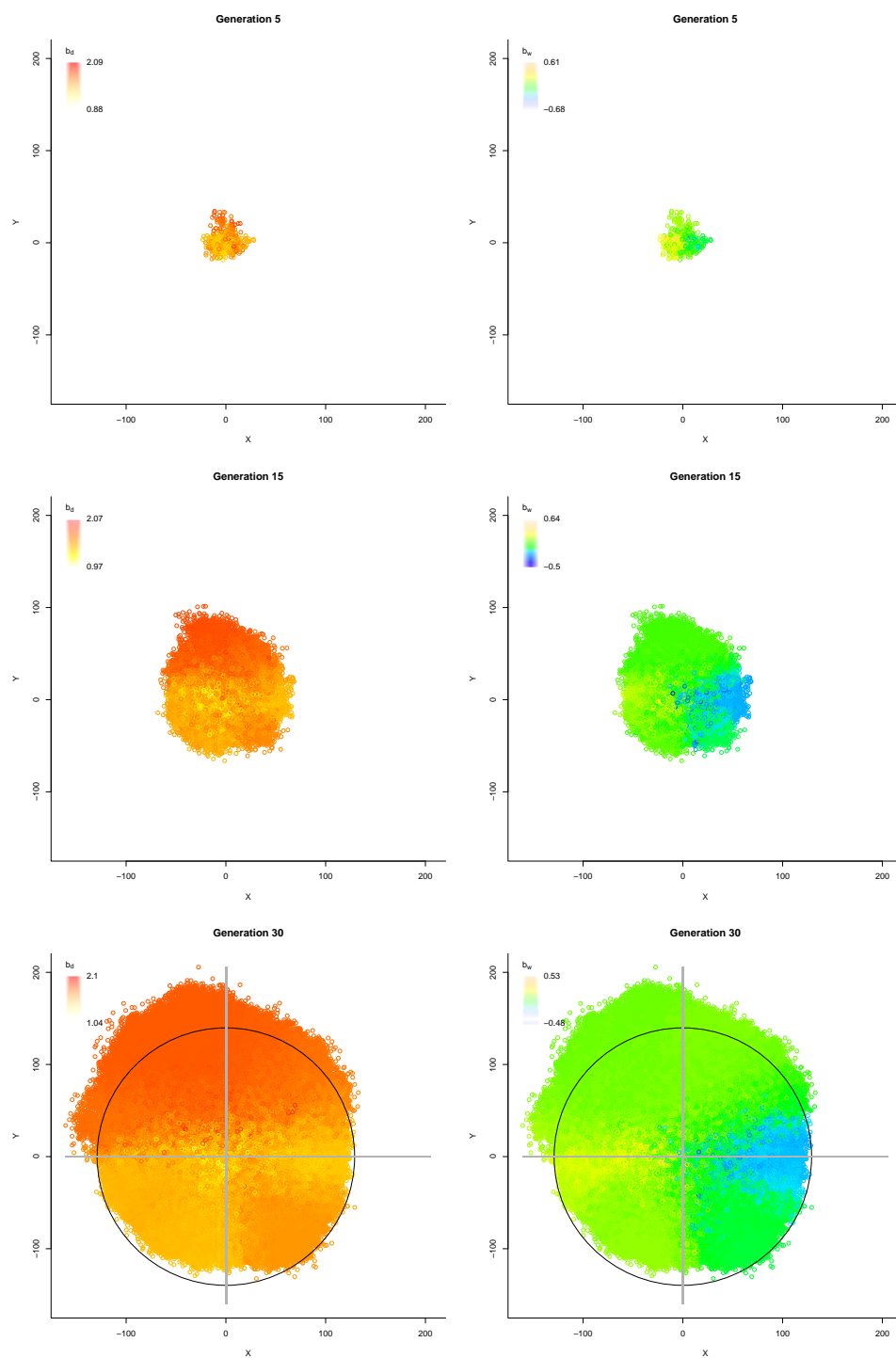
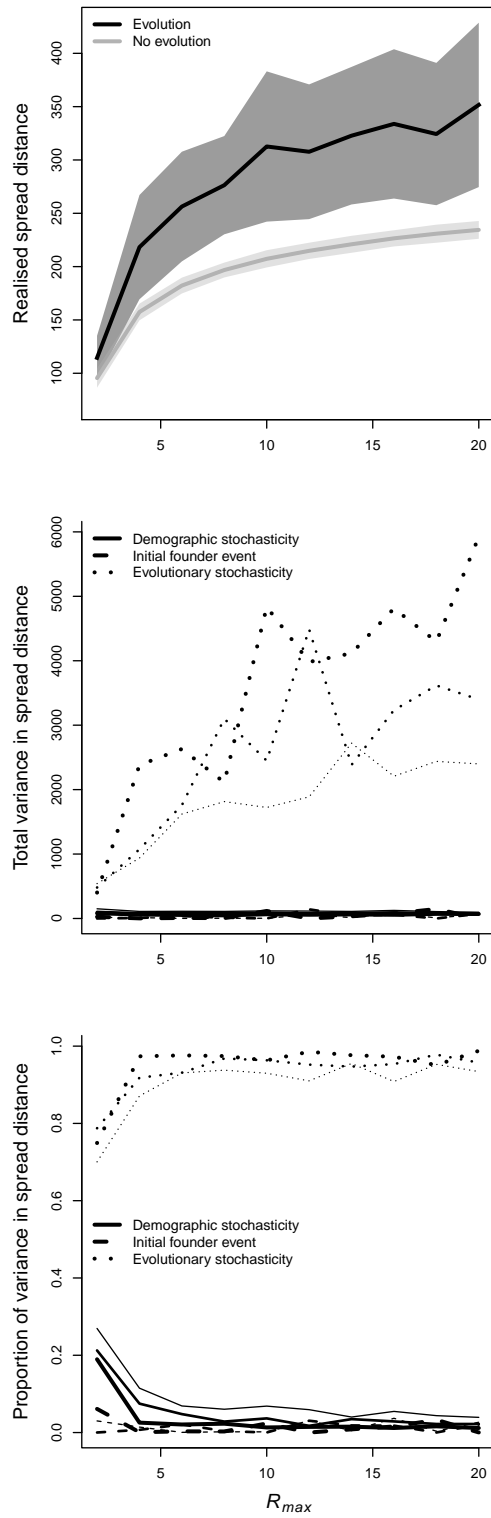
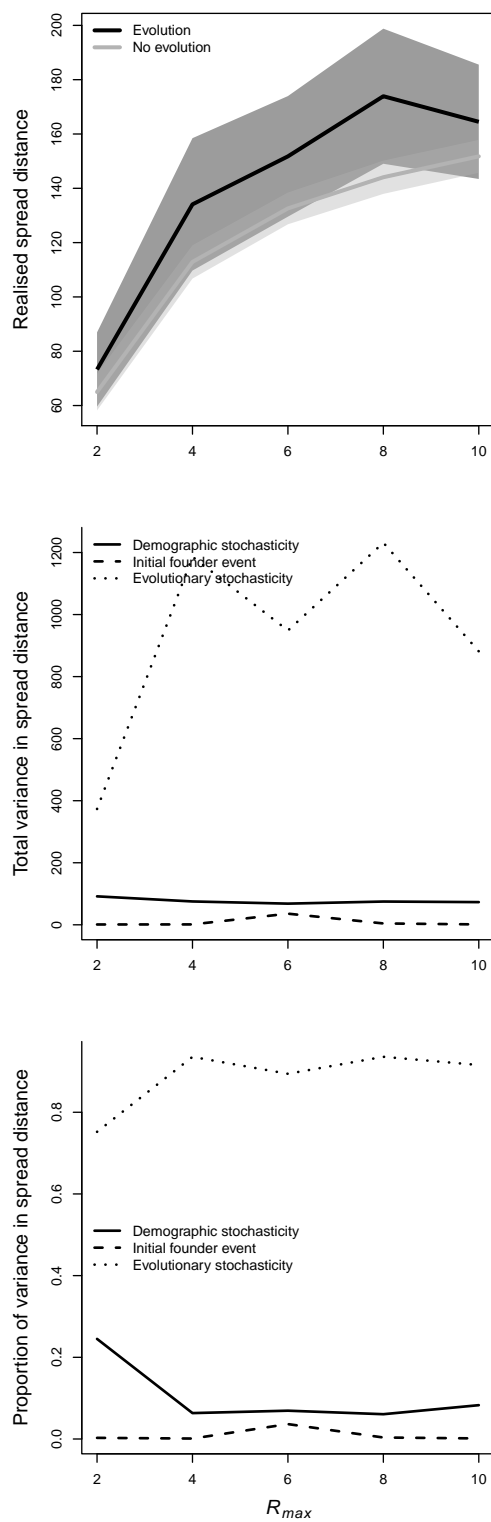


Figure 2:
35



36

Figure 3:



37

Figure 4: